Aqueous Solvation of *p*-Aminobenzonitrile in the Excited States: A Molecular Level Theory on Density Dependence

Daisuke Yokogawa,[†] Hirofumi Sato,*[,†] Shigeyoshi Sakaki,[†] and Yoshifumi Kimura[‡]

Department of Molecular Engineering, Graduate School of Engineering, Kyoto University, Kyoto 615-8510, Japan, and Department of Chemistry, Graduate School of Science, Kyoto University, Kyoto 606-8501, Japan

Received: October 30, 2009; Revised Manuscript Received: November 26, 2009

Osawa et al. recently studied density dependence of electronic absorption spectra of *p*-aminobenzonitrile (ABN) in supercritical and subcritical water. They reported the peak position exhibits a minimum in a specific density. RISM-SCF-SEDD, which is a combination method of ab initio electronic structure theory and a statistical mechanics for molecular liquids, was applied to address the origin of this challenging phenomena. Highly accurate electronic structure theories (CASSCF and MCQDPT2) coupled with microscopic description of hydrogen bonding were employed over a wide range of density condition. We found that the solvation effects on the lower two excited states show different density dependence, suggesting that the turnover is attributed to the difference in sensitivity to solvent of the two states.

Introduction

Ab initio molecular orbital (MO) theory is recognized as one of standard approaches to study the electronic structure of an isolated molecule. At the same time, popularization of hybrid-type theories such as polarizable continuum model (PCM), in which MO theory is combined with dielectric continuum model, has prompted us to rapidly step up understanding of a solvated molecule. Then a question may arise: how about the intermediate state between them? Supercritical fluids have been attracting much attention by their unique properties for chemical applications and various spectroscopic experiments have been performed so far. The present study is focusing on the electronic structure of molecule under a wide range of density of solvent.

In close connection with a photochemistry of 4-*N*,*N*-dimethylaminobenzonitrile (DMABN) in polar solvents, where the anomalous behavior observed in the fluorescence has attracted a lot of attention from the researchers, *p*-aminobenzonitrile (ABN) has been extensively studied both by experiments and computations.[1−12] Osawa et al. recently reported Raman spectra of the C≡N stretching vibration of ABN and its electronic absorption spectra in water, methanol, and cyclohexane under sub- and supercritical conditions as well as in acetonitrile under subcritical condition.[12] As the solvent density increases from the gaseous region to $\rho_r = 1.5$, where ρ_r is the reduced density by the critical density of the solvent, the absorption peak positions in water and methanol decrease. On the other hand, at the higher density region ($\rho_r > 2.7$), the absorption peak in water increases as the water density increases; that is, the spectra exhibits a minimum around $\rho_r \simeq 2.7$. It is conceivable that this interesting observation is attributed to the change in the electronic structure of ABN, but its mechanism still remains an open question.

In the past two decades, dielectric continuum model such as PCM and QM/MM method have been getting popular to study the electronic structure of solvated molecules. The electronic excitation of solvated molecules in the vicinity of standard thermodynamic condition have been studied based on these methods.[13] For example, Gao et al. correctly reproduced excited-state pK_a of phenol in aqueous solution.[14] Although a new attempt has just started to deal with pressure effect in the framework of continuum model,[15] it still seems difficult to apply the method to the present subject; i.e., dielectric constant and cavity radius are the parameters to represent the interaction between solute (ABN) and solvent, but their appropriate definition for sub- or supercritical condition might be questionable. If the statistically homogeneous treatment over a wide range of density is achieved, QM/MM is applicable to such a condition and reliable computational results are obtained.[16] A highly sophisticated electronic structure theory is also required to accomplish an adequate accuracy of the excitation energy in the absorption process.

Here, we present a theoretical study using the third method, RISM-SCF.[17] RISM-SCF is a combination method of ab initio MO theory and reference interaction site model (RISM),[18] which is a statistical mechanics for molecular liquids. Due to its inherent characteristic on the basis of algebraical treatment, RISM is essentially free from statistical error and allows us to study a wide range of thermodynamic conditions with uniform accuracy.[19,20] It is also important that a combination with high-level MO theories is realizable due to the lower computational demand of RISM. In the present study, the new generation of RISM-SCF, in which the spatial electron density distribution (SEDD) is explicitly treated, is employed. Because RISM-SCF-SEDD is numerically stable,[17] even if the buried atoms are involved in the solute molecule, the applicability to chemical reactions covered by this theory is very wide ranging compared to the original method.

It has been recognized that the theoretical treatment on the density dependency of excitation spectra is infeasible because a highly accurate electronic structure theory must be coupled with thermodynamic aspect related to an infinite number of solvent molecules. In particular, hydrogen bonding in aqueous solution necessitates the microscopic view. The background might refuse an approach such as dielectric continuum model or QM/MM method. To the best of our knowledge, this is the

* To whom correspondence should be addressed. E-mail: hirofumi@moleng.kyoto-u.ac.jp.
[†] Department of Molecular Engineering, Kyoto University.
[‡] Department of Chemistry, Kyoto University.

10.1021/jp910362z
Published on Web 12/29/2009

first report on the excitation spectra in aqueous solution over a wide range of density condition by utilizing a highly accurate ab initio theory.

Computational Method

All the computations were performed with the GAMESS program package[21] modified by us to implement the RISM-SCF-SEDD method. Since details of RISM-SCF and RISM-SCF-SEDD were reported in elsewhere,[17] we shall briefly explain the method. In RISM-SCF theory, total energy of the system ($\mathscr{A}$) is defined as follows:

$$\mathscr{A} = E_{\text{solute}} + \Delta\mu = E_{\text{isolated}} + E_{\text{reorg}} + \Delta\mu \qquad (1)$$

E_{solute} is total energy of the solute molecule (ABN) within the framework of ab initio MO theory including solvation effect. It is different from the total energy in gaseous phase (E_{isolated}) by E_{reorg}, which represents the distortion of electronic structure. In the theory, the electronic structure of ABN and the solvent structure are simultaneously obtained, where the influence of surrounding solvent is naturally taken into account. $\Delta\mu$ is solvation free energy and explicitly defined in RISM theory such as

$$\Delta\mu = k_{\text{B}}T\sum_{\alpha}\sum_{\gamma}\rho\int 4\pi r^2\,\mathrm{d}r\left[\frac{1}{2}h_{\alpha\gamma}(r)^2 - c_{\alpha\gamma}(r) - \frac{1}{2}c_{\alpha\gamma}(r)h_{\alpha\gamma}(r)\right] \qquad (2)$$

where k_{B} is Boltzmann constant and $h_{\alpha\gamma}(r)$ and $c_{\alpha\gamma}(r)$ are total and direct correlation functions, respectively. ρ and T represent thermodynamic condition that was set to the corresponding experimental values.[12] In the case of solvent water, the conditions were varied over a wide range of density and temperature, as follows:

$$(\rho_{\text{r}}, T) = (1.34, 669), (1.69, 669), (2.02, 633), (2.32, 583), (2.75, 473), (3.02, 373), (3.15, 297), (3.17, 273.15),$$

where ρ_{r} is the reduced density with respect to the critical density, $\rho = 0.010\,763\,372$ molecules/Å^3. These are called as condition 1, condition 2, ... condition 8, in the order of increasing density throughout the study. Computation in methanol solvent was also carried out at the density of 0.005147123 molecules/Å^3, corresponding to $\rho_{\text{r}} = 2.97$, and 296 K.

For the electrostatic solute−solvent interaction SEDD was explicitly dealt with in the present method; namely, solvent molecules feel the electrostatic field generated by the electron clouds of ABN. The repulsive part was described by the standard Lennard-Jones potential,[22] whose parameters are summarized in Table 1. The RISM equation was solved using standard hypernetted chain (HNC) closure.

The ABN geometries at each condition (isolated molecule, in methanol, and the condition from no. 1 to no. 8) were fully optimized using DFT (B3LYP) level of theory with cc-pVDZ basis set. Then state-specific complete active space self-consistent-field (CASSCF) and MC-QDPT2 were carried out under C_s symmetry. In CASSCF wave function, we chose nine active orbitals (three π and three π^* for the benzene ring, π and π^* for C≡N, and the lone pair in the amino group) and distributed 10 electrons in these active orbitals, followed by the perturbation computations (MC-QDPT2), in which nine (chemical core) orbitals were frozen. In the RISM-SCF-SEDD computations for the excited states, the convergence of RISM procedure were attained with respect to the wave function of the each state.

TABLE 1: Lennard-Jones Parameters

molecule	site	charge/|e|	σ/Å	ε/(kcal/mol)
ABN	N (cyano)	*a*	3.200	0.170
	N (amino)	*a*	3.250	0.170
	C (cyano)	*a*	3.650	0.170
	C (benzene)	*a*	3.550	0.070
	H (benzene)	*a*	2.420	0.030
	H (amino)	*a*	2.420	0.030
water	O	–0.820	3.166	0.155
	H	0.410	1.000	0.056
methanol	Me	0.265	3.775	0.207
	O	–0.700	3.070	0.170
	H	0.435	1.000	0.056

[a] Not assigned. The electrostatic interaction is determined by RISM-SCF-SEDD procedure.

TABLE 2: Vertical Excitation Energy and Dipole Moments in Gaseous Phase

	S_0	S_1 (1^1B_2)	S_2 (2^1A_1)	
Vertical Excitation Energy (in eV)				
CASSCF	0.00[a]	4.73	6.32	at DFT geometry
	0.00[b]	4.78	6.52	at CASSCF geometry
MC-QDPT2	0.00[c]	4.26	4.93	at DFT geometry
	0.00[d]	4.32	5.09	at CASSCF geometry
Gibson et al.[2]		4.15		0_0^0 transition
Serrano-Andrés et al.[5]		4.01	4.44	CASPT2[e]
Sobolewski et al.[6]		4.26	4.98	CASPT2
Parusel et al.[8]		4.27	5.13	STEOM
Dipole moment (in Debye)				
CASSCF	6.04	5.76	12.14	at DFT geometry
	5.69	5.47	11.80	at CASSCF geometry
MC-QDPT2	6.19	6.58	10.71	at DFT geometry
	5.83	6.23	10.34	at CASSCF geometry
Schuddeboom et al.[3]	6.6	8.0−8.5		
Serrano-Andrés et al.[5]	6.89	6.70	12.42	CASSCF[e]
Sobolewski et al.[6]	6.19	6.06	12.25	CASSCF
Parusel et al.[8]	6.81	7.61	11.61	STEOM
Borst et al.[9]	6.41	7.20		

[a] −377.599556 au. [b] −377.601692 au. [c] −378.754131 au. [d] −378.751058 au. [e] $\theta = 0$ with 0° wagging angle.

Results and Discussion

Excitation Energy. In spectra shown by Khalil et al.,[1] a peak in the UV region (^1L_a) and a shoulder (^1L_b) were assigned, respectively corresponding to S_2 (A′) and S_1 (A″) states, because $S_1 \leftarrow S_0$ is an allowed transition. The computational results of the vertical excitation energy in the gaseous phase are summarized in Table 2. CASSCF computations give reliable energies, but they are steadily improved using the perturbation method. It is noted that several geometrical structures were examined in the previous studies with respect to the wagging motion or twisted angle of the amino group, and their excitation energies show slight geometry dependence. At any rate, the present results show good agreement with both of the experiments and previous computations. As pointed out by previous studies,[8,10] S_1 state is characterized as a mixture of various $\pi\pi^*$ transitions. It is noteworthy that S_1 and S_2 states are quite closely located and the energy gap is about 15 kcal/mol in gaseous phase.

Electronic structure is characterized by dipole moment. 6.04, 5.76, and 12.14 D were respectively obtained for the three states by CASSCF wave function (see Table 2). Borst et al. reported

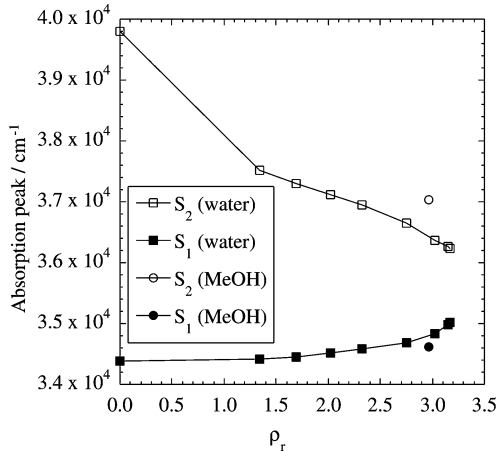

Figure 1. Excitation energy of ABN against the reduced density of the solvent.

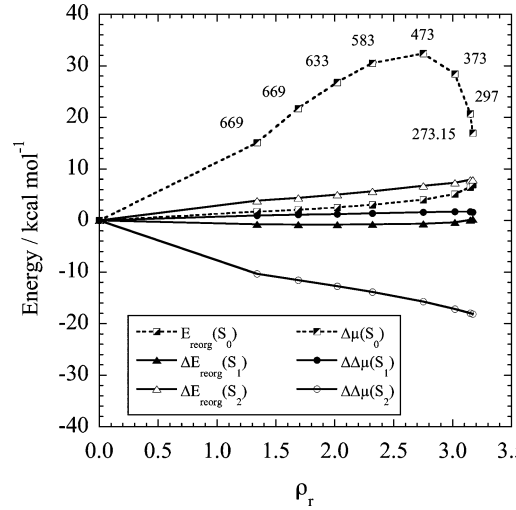

Figure 2. Energy components of the total energy of the system ($\mathcal{A}$) in aqueous solution. Dashed lines indicate the values for S_0 state, while solid lines are the difference from the ground state. The numbers shown are temperatures in K.

estimations of 6.41 (S_0) and 7.20 ± 0.3 (S_1) D based on the vector sum of bond dipole moments using information from electronic spectra.[9] Schuddeboom et al. also presented the dipole moments in nonpolar solvents, 6.6 (S_0), 8.0−8.5 (S_1) D.[3] The values for the electronic ground state are in reasonable agreement. Meanwhile the computation of $^1B_1$ state by CASSCF wave function somewhat underestimates the experimental one. We further checked the effect of the perturbation on the dipole moment using the finite-differential technique of electric field, which obviously increases the values. The present estimation looks reasonable compared to the previous computations, although they do not taken into account the dynamical correlation effect. According to the data, the dipole moments in the two excited states considerably depend upon the molecular geometry. Much higher level computation seems to be necessary to accurately evaluate the dipole moment in the excited states, but the present computational level is adequate enough to describe the electronic structure of the excited states in semiquantitative sense.

Density Dependence of Excitation Energy. In solution, the peak of absorption band is shifted to around 4.7−4.8 eV.[12,23] Figure 1 is a key result of the present study, the energy differences of S_1-S_0 and S_2-S_0 as functions of reduced density, corresponding to the vertical excitation energy in solvent. The left-hand side of the graph ($\rho_r = 0$) indicates the vertical excitation in gaseous phase. On increasing the density, the excitation energy to S_1 state gradually increases while that to S_2 state shows drastic decrease. The S_2 result looks very similar to the report by Osawa et al., and the peak shift is quantitatively reproduced in lower density region. On the other hands, a noticeable difference from the experimental observation appears in the high density region. In their report, a minimum was found around $\rho_r \simeq 2.7$, while the present result shows a monotonic decrease. Generally speaking, the computation requires input parameters (T and ρ_r) to specify the conditions and it is known that they are often deviated from the thermodynamic state in reality. It cannot be denied that the minimum is located at a much higher density region.

However, it is important to point out that S_1 evidently increases at the high-density region. Hence the following explanation may be possible. The observed absorption spectra[12] is essentially attributed to the shift in the S_2 state, but the shift in the S_1 state could affect the peak position of the UV-absorption band, too. Actually, the energy gap between them is getting smaller especially in the higher density region. Because of the difficulty in theoretical evaluation of the spectral bandwidth of the solvated molecule, further computations directly approaching the experimental observation are not feasible at this moment. In the figure, the computational result for methanol solvent is also depicted, where the shift in S_2 state, with respect to the aqueous environment, is properly reproduced.

From the definition of total energy, the excitation energy is given by

$$\Delta\mathcal{A} = \Delta E_{\text{isolated}} + \Delta E_{\text{reorg}} + \Delta\Delta\mu \qquad (3)$$

where $\Delta E_{\text{isolated}}$ is computed by the standard ab initio MO method; it is nothing but the vertical excitation energy of isolated molecule as listed in Table 2, being a constant value. The two dashed lines in Figure 2 are E_{reorg} and $\Delta\mu$ of ABN in the ground state. The curve of $\Delta\mu(S_0)$ might look peculiar in the high-density region, but it is presumably attributed to the immoderate temperature change. Further detailed analysis suggests that this profile comes from the solvation of the benzene ring. Remember that only the differences between the excited states and ground state (solid lines) get engaged to the absorption spectra. If the variations of the two different states along the density were exactly the same, the spectra do not show any dependency. As seen in the figure, $\Delta\Delta\mu(S_2)$ exhibits remarkable density dependence, indicating that the solvation in S_2 state is very different from that in the ground state. The contribution from $\Delta E_{\text{reorg}}(S_2)$ is not so large, and hence the change in solvation, $\Delta\Delta\mu(S_2)$, should be responsible for the main red shift in the absorption spectra. In S_1, both of the contributions are relatively small, suggesting the similarities in solvation phenomena to the ground state. The rise found in the high-density region (1) should be associated with $\Delta E_{\text{reorg}}(S_1)$ because $\Delta\Delta\mu(S_1)$ barely decreases at this region. As described above, the contribution is originated from the distortion of the electronic structure in ABN. Compared to the ground state, S_1 state receives greater influence from the solvent at the higher density environment. It is noted that all the differences (ΔE_{reorg} and $\Delta\Delta\mu$) show virtually monotonic variations and any specific behavior is not found in respective contributions. The experimentally observed anomalous feature in the spectra is ascribed as the cause of an interplay among these multiple contributions.

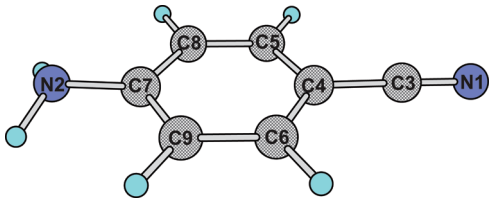

Figure 3. ABN molecule with atomic index. Hydrogen atoms attaching to C5 and C6 are H8 and H9, and those to C8 and C10 are H11 and H12. The amino hydrogen atoms are H14 and H15.

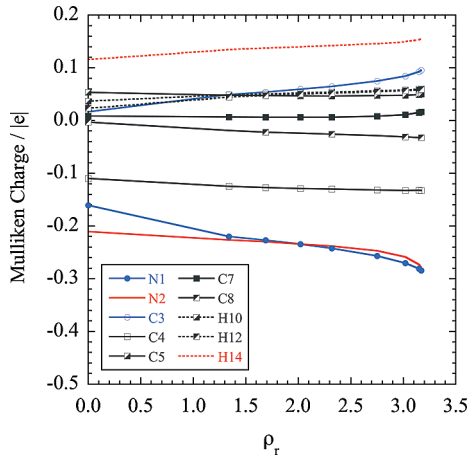

Figure 4. Mulliken change of S_0 against the reduced density of the solvent. See Figure 3 for the atomic index.

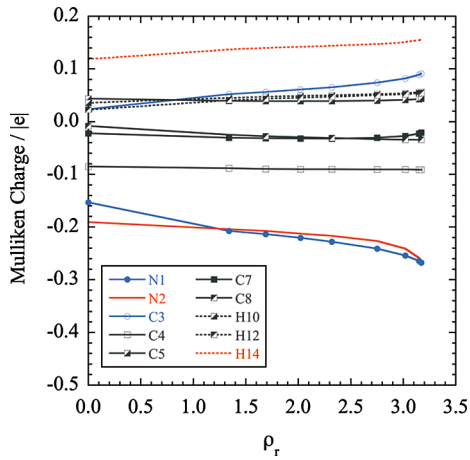

Figure 5. Mulliken change of S_1 against the reduced density of the solvent.

Charge Distribution. The electronic structure is strongly affected by solvation. Figures 4, 5, and 6 represent the change of Mulliken charges computed from CASSCF wave functions. As expected, nitrogen atom in cyano group is always negatively charged and the electron population increases as density increases. At the same time, the attached carbon atom becomes positively charged. The change in amino group is much more moderate, but the N−H bond polarization is gradually enhanced by the increasing density. The most dramatic dependency is found in S_2 state (Figure 6). Even in the gaseous phase, the cyano nitrogen atom is negatively charged while the amino group loses electrons, corresponding to the CT character. As density increases, the cyano group further draws electrons. In contrast, the S_1 state looks very similar to the change in the ground state. As mentioned above, the state is characterized by $\pi\pi^*$ transitions, which is localized on the benzene ring, and the solvent effect on the electronic structure is relatively small.

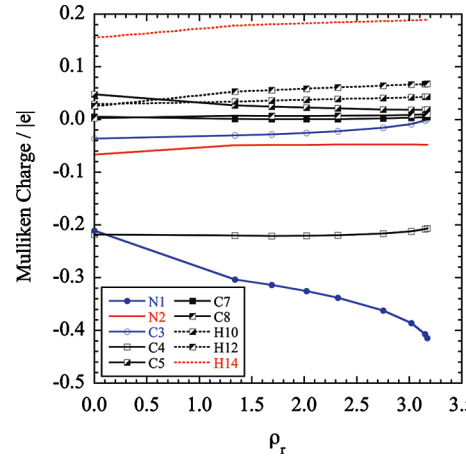

Figure 6. Mulliken change of S_2 against the reduced density of the solvent.

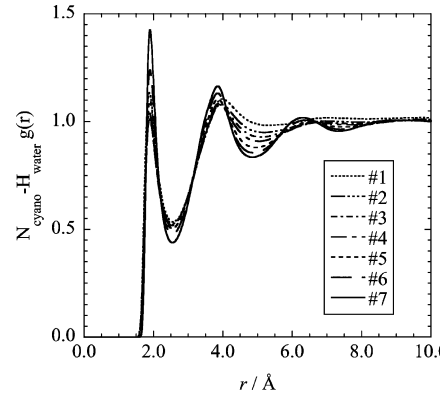

Figure 7. Pair correlation function between N(cyano)−H(water).

The same discussion can be applied to the dipole moment and its changes. The magnitude of the dipole-moment change in the S_2 state is nearly 3 times greater than the other two states, while that in S_1 is slightly little compared to the ground state. As a consequence, the relative values for the two excited states are in opposite directions, which is consistent with the shift in the excitation energy.

Solvation Structure. In analyzing partial charges assigned to each atom in the ground state, the nitrogen atoms in the cyano group as well as in the amino group get negatively charged as the density increases. It is natural to consider that solvation structure around the groups should change as the density. Figure 7 shows the pair correlation function between nitrogen in the cyano group and water hydrogen. Figure 8 shows that between nitrogen in the amino group and the hydrogen. Both of them show typical hydrogen-bonding character: a sharp peak is found around $r = 2.0$ Å, and the paired water hydrogen atom is found as the second broad peak ($r \simeq 4.0$ Å). All the peak positions are hardly affected by the density difference, but their heights show the clear dependency. At the low-density region, all the peaks, especially beyond the second ones, tend to be broaden and the profile of the correlation function look similar to that in gaseous phase. On the contrary, the peaks become distinct at the high-density region.

To examine the change of the solvation structure, coordination number ($N_{\alpha\gamma}$) is calculated by the standard definition.

$$N_{\alpha\gamma} = \rho_\gamma \int_0^{r_{\min}} g_{\alpha\gamma}(r) 4\pi r^2 \, dr \qquad (4)$$

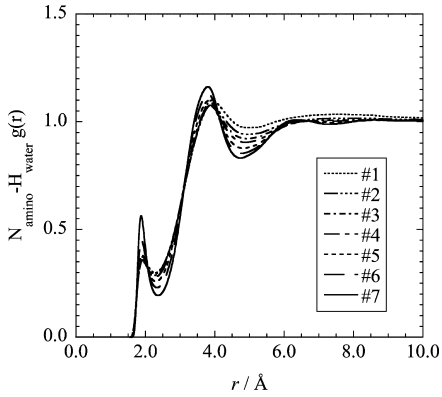

Figure 8. Pair correlation function between N(amino)−H(water).

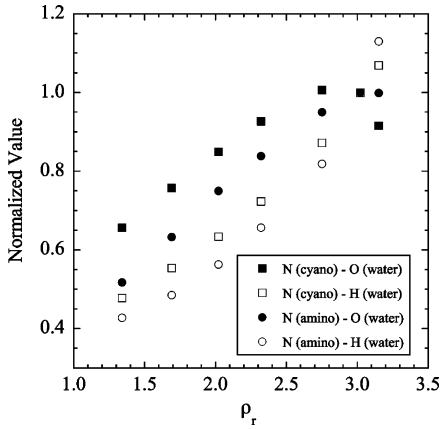

Figure 9. Change of coordination number around the cyano and amino groups evaluated from pair correlation function. Values are scaled so as to be normalized at $\rho_r = 3.02$.

where r_{min} was set to the minimum point just after the first peak. Osawa et al. reported normalized $N_{\alpha\gamma}$ obtained by molecular dynamics simulation as a function of density. Figure 9 displays the same quantity but computed from the present method, in which solute electronic structure related to the solute−solvent electrostatic interaction is determined in a self-consistent manner. As they pointed out, the change is rather monotonical over a wide range of density. Since the coordination number of the solvent increases with increasing density, the electric field generated by solvent water is also intensified monotonically. Interestingly, the contribution from water oxygen seems to be saturated around $\rho_r \simeq 3.0$ while that from hydrogen seems to continue to increase. This is because the hydrogen atom in water is virtually embedded in the oxygen; the radius of the oxygen ($\sigma/2$) is longer than the O−H bond length. In aqueous solution, hydrogen bonding is primary important to determine the liquid structure in the intermediate-density region but it is gradually replaced with packing effect in the high-density region.[19] Water oxygen is stuffed to directly contact to the nitrogen atom until it is fully packed. Even in this situation a water is still allowed to rotate and the hydrogen atom can take preferential orientation.

Conclusions

RISM-SCF-SEDD, which is a combination method of ab initio electronic structure theory and a statistical mechanics for molecular liquids, was applied to address the origin of the turn over found in the *p*-aminobenzonitrile (ABN) system, which was reported by Osawa et al. Highly accurate electronic structure theories (CASSCF and MCQDPT2) coupled with microscopic description of hydrogen bonding were employed over a wide range of density condition. We found that the solvation effects on the lower two excited states show different density dependence, suggesting that the turnover is attributed to the difference in sensitivity to solvent of the two states. In aqueous solution, hydrogen bonding is primarily important to determine the liquid structure in the intermediate-density region but it is gradually replaced with packing effect in the high-density region. The shift in the spectra is also related to this complex transit.

Osawa et al. reported the Raman spectra of the C≡N stretching vibration of ABN and reported another interesting phenomena. Since the vibrational spectra are also affected by the solvation, a new theory that can deal with the vibrational spectra of a solvated molecule is necessary. The dynamical feature of phenomenon becomes considerably important to evaluate reliable spectra of a solvated molecule. We are pursuing efforts for the fulfillment of this requirement.

Acknowledgment. This work has been financially supported by the Grant-in-Aid for Scientific Research (B) (19350010) supported by the Japan Society for the Promotion of Science (JSPS).

References and Notes

(1) Khalil, O. S.; Meeks, J. L.; McGlynn, S. P. *Chem. Phys. Lett.* **1976**, *39*, 457.
(2) Gibson, E. M.; Jones, A. C. *Chem. Phys. Lett.* **1988**, *146*, 270.
(3) Schuddeboom, W.; Jonker, S. A.; Warman, J. M.; Leinhos, U.; Kuehnle, W.; Zachariasse, K. A. *J. Phys. Chem.* **1992**, *96*, 10809.
(4) Howells, B. D.; McCombie, J.; Palmer, T. F.; Simons, J. P.; Walters, A. *J. Chem. Soc., Faraday Trans.* **1992**, *88*, 2595.
(5) Serrano-Andrés, L.; Merchán, M.; Roos, B. O.; Lindh, R. *J. Am. Chem. Soc.* **1995**, *117*, 3189.
(6) Sobolewski, A. L.; Domcke, W. *Chem. Phys. Lett.* **1996**, *250*, 428.
(7) Lommatzsch, U.; Brutschy, B. *Chem. Phys.* **1998**, *234*, 35.
(8) Parusel, A. B. J.; Köhler G.; Nooijen, M. *J. Phys. Chem. A* **1999**, *103*, 4056.
(9) BorstD., R.; Korter, T. M.; Pratt, D. W. *Chem. Phys. Lett.* **2001**, *350*, 485.
(10) Ma, C.; Kwok, W. M.; Matousek, P.; Parker, A. W.; Phillips, D.; Toner, W. T.; Towrie, M. *J. Phys. Chem. A* **2002**, *106*, 3294.
(11) Dahl, K.; Biswas, R.; Ito, N.; Maroncelli, M. *J. Phys. Chem. B* **2005**, *109*, 1563.
(12) Osawa, K.; Hamamoto, T.; Fujisawa, T.; Terazima, M.; Sato, H.; Kimura, Y. *J. Phys. Chem. A* **2009**, *113*, 3143.
(13) (a) Cammi, R.; Mennucci, B.; Tomasi, J. *J. Phys. Chem. A* **2000**, *104*, 5631. (b) Mennucci, B.; Toniolo, A.; Tomasi, J. *J. Am. Chem. Soc.* **2000**, *122*, 10621. (c) Caricato, M.; Ingrosso, F.; Mennucci, B.; Tomasi, J. *J. Chem. Phys.* **2005**, *122*, 154501. (d) Mennucci, B.; Cappelli, C.; Guido, C. A.; Cammi, R.; Toniolo, A.; Tomasi, J. *J. Phys. Chem. A* **2009**, *113*, 3009.
(14) Gao, J.; Li, N.; Freindorf, M. *J. Am. Chem. Soc.* **1996**, *118*, 4912.
(15) Cammi, R.; Verdolino, V.; Mennucci, B.; Tomasi, *J. Chem. Phys.* **2009**, *334*, 135.
(16) Lin, Y.-l.; Gao, J. *J. Chem. Theor. Comput.* **2007**, *3*, 1484.
(17) (a) Ten-no, S.; Hirata, F.; Kato, S. *J. Chem. Phys.* **1994**, *100*, 7443. (b) Sato, H.; Hirata, F.; Kato, S. *J. Chem. Phys.* **1996**, *105*, 1546. (c) Yokogawa, D.; Sato, H.; Sakaki, S. *J. Chem. Phys.* **2007**, *126*, 244054.
(18) (a) Chandler, D.; Andersen, H. C. *J. Chem. Phys.* **1972**, *57*, 1930. (b) Hirata, F.; Rossky, P. J. *Chem. Phys. Lett.* **1981**, *83*, 329.
(19) Sato, H.; Hirata, F. *J. Chem. Phys.* **1999**, *111*, 8545.
(20) (a) Sato, H.; Hirata, F. *J. Phys. Chem. A* **1998**, *102*, 2603. (b) Sato, H.; Hirata, F. *J. Phys. Chem. B* **1999**, *103*, 6596. (c) Yoshida, N.; Ishizuka, R.; Sato, H.; Hirata, F. *J. Phys. Chem. B* **2006**, *110*, 8451.
(21) Schmidt, M. W.; et al. *J. Comput. Chem.* **1993**, *14*, 1347.
(22) (a) Jorgensen, W. L.; Laird, E. R.; Nguyen, T. B.; Tirado-Rives, J. *J. Comput. Chem.* **1993**, *14*, 206. (b) Sato, H.; Kobori, Y.; Tero-Kubota, S.; Hirata, F. *J. Chem. Phys.* **2003**, *119*, 2753.
(23) Zachariasse, K. A.; von der Haar, T.; Hebecker, A.; Leinhos, U.; Kuhnle, W. *Pure Appl. Chem.* **1993**, *65*, 1745.
(24) Lippert, *Ber. Bunsenges. Phys. Chem.* **1979**, *83*, 692.

JP910362Z